

Dedicated to Prof. Dorin N. Poenaru's
70th Anniversary

BINARY AND TERNARY FISSION WITHIN STATISTICAL APPROACH

A.V. ANDREEV^{1,2}, G.G. ADAMIAN^{1,3}, N.V. ANTONENKO^{1,2},
S.P. IVANOVA¹, W. SCHEID²

¹Joint Institute for Nuclear Research, 141980 Dubna, Russia

²Institut für Theoretische Physik der Justus-Liebig-Universität
D-35392 Giessen, Germany

³Institute of Nuclear Physics, Tashkent 702132, Uzbekistan

(Received February 25, 2007)

Abstract. Binary fission observables are described within the scission-point model by calculating the potential energy with the dinuclear system model. For the description of ternary fission we extend the scission-point model of binary fission. The ternary system with a light nucleus between two heavy fragments is assumed to be formed from the binary configuration near to the scission point. Charge number distributions, mean total kinetic energies and neutron multiplicity distributions are treated and compared with the experimental data for binary fission of actinides and for ternary fission of ^{252}Cf accompanied by different light charged particles.

Key words: binary fission, dinuclear system, ternary fission, scission point model.

1. INTRODUCTION

The process of nuclear fission and cluster radioactivity was and is intensively investigated by experimentalists and theorists. Poenaru *et al.* were the first who predicted the cluster radioactivity before this decay was found in experiment (see [1] and [2]). Despite of the large theoretical efforts, our knowledge of the fission process is far from completeness and should be extended further.

Among various models, the scission-point model [3] together with the dinuclear system (DNS) concept [4] provides a quite simple and clear mechanism for the description of fission. The present work is devoted to the description

of binary fission using the scission-point model and dinuclear system concept. The ternary fission is described in an analogous manner.

We consider the fission of heavy nuclei from Th to No. There exists detailed experimental information on the fission characteristics in this region [5–14]. Masses and charges of fission fragments, their kinetic energies, the number of neutrons emitted from the fragments after the decay were measured. In the last two decades there were many experiments [15–20] carried out on the spontaneous ternary fission of ^{252}Cf . The study of these rare processes is a challenge for the theory and is important for the understanding of the fission mechanism. Due to the emission of a light charged particle (LCP) from the region between the two heavy fragments, the process of the formation of fission fragments near the scission point becomes observable and the nuclear shape at the scission point can be explored. Based on the experimental information, it has been suggested in Ref. [21] that the ternary fission is a particular case of binary fission, i.e. the LCP is formed in the process of binary fission. The microscopic study [22] of the formation probability of an alpha-particle in the fissioning nucleus supports the hypothesis of the formation of an alpha-particle between the heavy fragments in the last stage of the fission process. The same conclusion follows from classical and semiclassical dynamical and statistical treatments [23–26]. In the present work we consider the formation of the ternary system as the second step after the formation of the binary system.

In Section 2 we consider the method of the calculation of the potential energy of binary and ternary scission configurations. Section 3 contains the results of the calculations of charge distributions, mean TKE-mass distributions and neutron multiplicity distributions for both binary and ternary fission processes. A summary is given in Section 4.

2. POTENTIAL ENERGY OF THE SCISSION CONFIGURATION

2.1. BINARY SYSTEM

In the binary fission the fissioning nucleus with the mass number A and charge number Z is modeled near the scission point by the dinuclear system consisting of two co-axial nearly touching axially symmetric prolate deformed ellipsoids. The geometry of this binary system is described with the set of parameters: the mass numbers A_i and charge numbers Z_i of the fragments ($i = 1, 2$), the deformation parameters of the fragments β_i , and the distance d between the centers of the fragments. To describe the deformation of the fragments, the ratio of major (c_i) and minor (a_i) semi-axes of the ellipsoid

was chosen as deformation parameter $\beta_i = c_i/a_i$. The volume conservation condition is taken into account. A schematic picture of the binary system with the parameters is presented in Fig. 1.

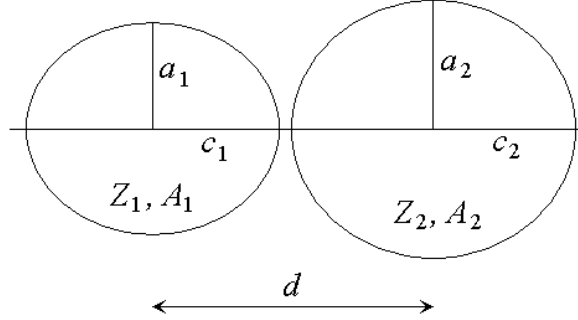


Fig. 1 – Schematic picture of a binary system with the parameters describing its geometry.

In the scission-point model the probabilities of formation of different scission configurations depend on the value of the potential energy of the system at the scission point. The general expression for the potential energy of a binary system consists of the following terms: the binding energies of the individual fragments, the energy of interaction between the DNS fragments and the rotational energy of the system:

$$\begin{aligned}
 U(\{A_i, Z_i, \beta_i\}, d, L) &= U_1^{LD}(A_1, Z_1, \beta_1) + \delta U_1^{sh}(A_1, Z_1, \beta_1) \\
 &+ U_2^{LD}(A_2, Z_2, \beta_2) + \delta U_2^{sh}(A_2, Z_2, \beta_2) \\
 &+ V^{C,int}(\{A_i, Z_i, \beta_i\}, d) + V^{N,int}(\{A_i, Z_i, \beta_i\}, d) \\
 &+ V^{rot}(\{A_i, Z_i, \beta_i\}, d, L), \tag{1}
 \end{aligned}$$

where L is the angular momentum of the system. The energy of the i -th fragment consists of the liquid-drop energy U_i^{LD} and the microscopic shell correction term δU_i^{sh} . The liquid-drop energy is calculated by using the parameters of Ref. [27]. The shell correction term is calculated in the Strutinsky prescription [28] by using the two-center shell model [29]. The interaction potential consists of the Coulomb interaction $V^{C,int}$ and nuclear interaction $V^{N,int}$. The first interaction is calculated with uniformly charged ellipsoids, while the second one with a double-folding of nuclear densities with density-dependent Skyrme-type delta-forces [30]. For spontaneous and neutron induced fission we take $V^{rot} = 0$.

For a particular binary system at fixed fragment deformations the interaction potential is a function of the distance between the two binary fragments. The nuclear interaction has a minimum as a function of the distance, i.e. it

is attractive for large distances and repulsive for small distances. As result of the summation of the different potentials, we find a potential with a minimum which we call “potential pocket” (Fig. 2). The depth of this minimum depends on the masses and deformations of the interacting nuclei. The depth is larger for light nuclei and smaller for heavy ones. With increasing deformations the depth of the potential pocket decreases. For very heavy fragments, for example, in the fission of nuclei heavier than ^{262}No into a symmetrical fragmentation, there is no potential pocket at any deformations of the fragments. For lighter nuclei like U, Pu, Cf the potential pocket can exist for small deformations but disappears for larger ones. If the fragments are light, the pocket exists at any reasonable deformation. The barrier resulting from our calculations is consistent with the existence of third minima found experimentally [31] in some heavy nuclei and with the shell model and macroscopic-microscopic calculations [32]. It was already earlier mentioned in Ref. [33] that the qualitative reason for such a third well is the complete formation of the fragments at the scission point.

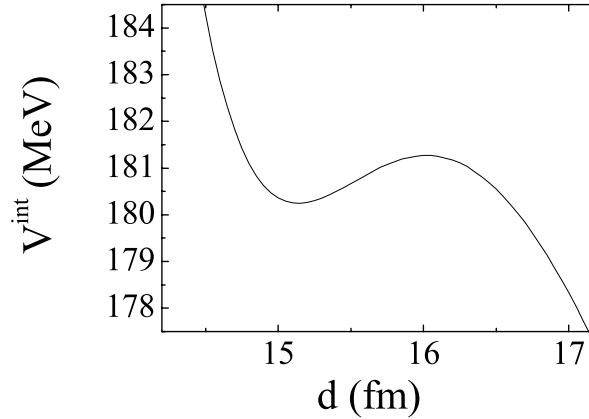


Fig. 2 – The interaction potential as a function of the distance between the fragments for the system $^{235}\text{U}(n_{th}, f) \rightarrow ^{102}\text{Zr} + ^{134}\text{Te}$. The deformations $\beta_1 = 1.75$ and $\beta_2 = 1.2$ are taken at the minimum of the potential energy surface. The masses and charges of the fragments are taken at the maximum of the distribution of the fission fragments.

Due to the potential pocket the binary system lives some time before fission. The potential barrier prevents the system from immediate decay. During this time the system achieves equilibrium between the collective and internal degrees of freedom. This fact allows us to use the statistical approach for the calculation of different characteristics of fission which are mostly determined

2.2. TERNARY SYSTEM

For the description of ternary fission we developed a model similar to the DNS model for binary fission. The ternary system near scission is modeled by three co-axial ellipsoids: two heavy fragments 1 and 2, and the light fragment 3 between them (Fig. 4). The parameters of the system are the masses, charges and deformations of the three fragments and the distances d_1 and d_2 between the fragments. The potential energy of the ternary system, consisting of the fragments with (Z_1, A_1) , (Z_2, A_2) and (Z_3, A_3) , is defined analogously to the binary case as follows

$$\begin{aligned} U(\{A_i, Z_i, \beta_i, d_i\}, L) &= U_1^{LD}(A_1, Z_1, \beta_1) + \delta U_1^{sh}(A_1, Z_1, \beta_1) \\ &+ U_2^{LD}(A_2, Z_2, \beta_2) + \delta U_2^{sh}(A_2, Z_2, \beta_2) + U_3(A_3, Z_3) \\ &+ V^{int}(\{A_i, Z_i, \beta_i, d_i\}) + V^{rot}(\{A_i, Z_i, \beta_i, d_i\}, L), \end{aligned} \quad (2)$$

with

$$\begin{aligned} V^{int}(\{A_i, Z_i, \beta_i, d_i\}) &= \\ &= V_{12}^C(A_1, Z_1, A_2, Z_2, \beta_1, \beta_2, d_1 + d_2) + V_{12}^N(A_1, Z_1, A_2, Z_2, \beta_1, \beta_2, d_1 + d_2) \\ &+ V_{13}^C(A_1, Z_1, A_3, Z_3, \beta_1, \beta_3, d_1) + V_{13}^N(A_1, Z_1, A_3, Z_3, \beta_1, \beta_3, d_1) \\ &+ V_{23}^C(A_2, Z_2, A_3, Z_3, \beta_2, \beta_3, d_2) + V_{23}^N(A_2, Z_2, A_3, Z_3, \beta_2, \beta_3, d_2). \end{aligned} \quad (3)$$

We consider only a light third fragment up to oxygen. Hence, the third fragment is stiff and its potential energy U_3 is taken at the fixed deformation of the ground state of the nucleus with (A_3, Z_3) . The parameters of radii r_0 (in fm) are set to 1.03 for ${}^4\text{He}$, 1.12 for ${}^{8,10}\text{Be}$, and 1.15 for other nuclei.

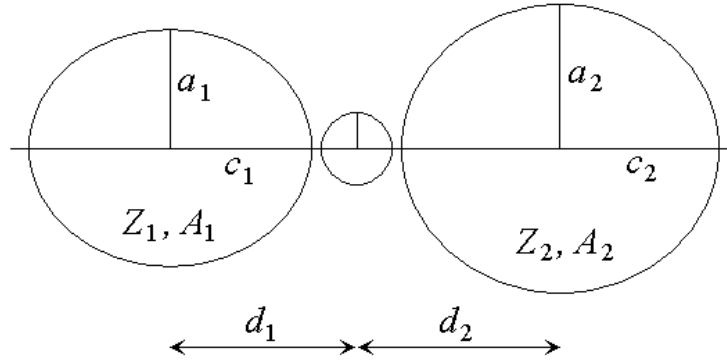


Fig. 4 – Schematic picture of the ternary system with the parameters describing its geometry (the parameters of the third particle are not shown).

At fixed deformations of the fragments the interaction potential is a function of two distances d_1 and d_2 . The potential is the sum of three Coulomb and three nuclear interactions in the three pairs of the fragments. The term V_{12}^N is negligible because the overlapping of the nuclear densities of the fragments 1 and 2 is small. At fixed deformations of the fragments the interaction potential has a minimum as a function of d_1 and d_2 near to the touching distances. Like in the binary case we need to calculate the potential energies for the distances d_1 and d_2 corresponding to the barrier of the interaction potential. The height of the barrier is about 1 MeV and depends on the particular way from the minimum to the barrier in the (d_1, d_2) -space. But this dependence is small. For the calculations we chose the relation $A_1 d_1 = A_2 d_2$, corresponding to the case when the third particle stays at rest in the center-of-mass coordinate system.

Since the deformation of the third fragment is fixed, the potential energy surface can be drawn for the ternary system as a function of β_1 and β_2 analogously to the binary case. In ternary systems the distance between the heavy fragments is larger than in the binary ones and, therefore, the Coulomb interaction is smaller. Hence, the deformations of the fragments in ternary systems are, in general, smaller than those in binary systems.

3. RESULTS OF THE CALCULATIONS

3.1. RELATIVE CHARGE DISTRIBUTIONS

3.1.1. Binary fission

The statistical approach allows us to calculate the yields of different binary system configurations by using the potential energy of the system at the scission point. The probability of formation of the system with mass and charge numbers of the fragments (A_1, Z_1) and (A_2, Z_2) at some deformations β_1 and β_2 is proportional to the Boltzmann factor

$$w(A_1, Z_1, \beta_1, A_2, Z_2, \beta_2, E^*) \propto \exp \left[-\frac{U(A_1, Z_1, \beta_1, A_2, Z_2, \beta_2, E^*)}{T} \right], \quad (4)$$

where T is the temperature of the system. It depends on the excitation energy and can be estimated by using the expression $T = (E^*/a)^{1/2}$, where a is the level density parameter. For the present calculations we chose the value $a = A/12 \text{ MeV}^{-1}$ which was used for the description of fusion [34]. The excitation energy is calculated as the initial one of the fissioning nucleus plus the difference between the potential energy of the fissioning compound nucleus and the potential energy of the system at the scission point. For the calculation

of the temperature of the system the value of excitation energy is taken in the deepest minimum of the potential energy surface.

If one needs to calculate the relative yield of a certain system regardless of the deformation parameters, this probability should be integrated over the deformations:

$$Y(A_1, Z_1, A_2, Z_2, E^*) = Y_0 \int \int \exp \left[-\frac{U(A_1, Z_1, \beta_1, A_2, Z_2, \beta_2, E^*)}{T} \right] d\beta_1 d\beta_2, \quad (5)$$

where Y_0 is the normalization factor. It should be noted that the statistical approach does not allow to calculate the absolute values of the yields; one just obtains the relative yields of the systems. Since the temperatures of the systems considered here are about 1 MeV, only deformations near to the minima give significant contributions to the probabilities and yields.

In order to obtain the charge distributions one has to sum the expression (5) over the mass number A_1 of the fragments

$$Y(Z_1) = Y_0 \sum_{A_1} \int \int \exp \left[-\frac{U(A_1, Z_1, \beta_1, A_2, Z_2, \beta_2, E^*)}{T} \right] d\beta_1 d\beta_2. \quad (6)$$

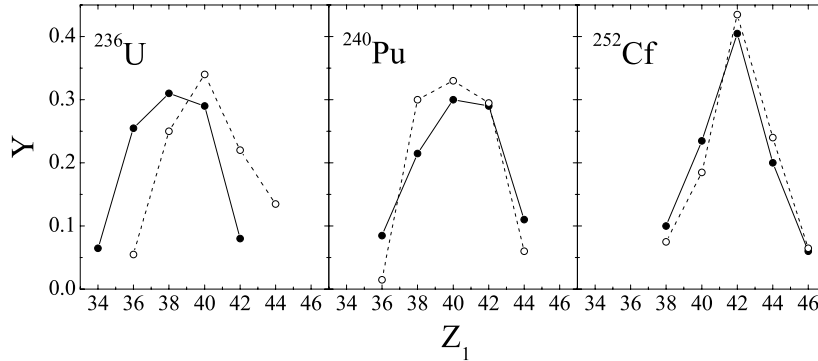


Fig. 5 – Comparison of calculated and experimental charge number distributions for neutron induced fission of ^{236}U and ^{240}Pu , and spontaneous fission of ^{252}Cf . The experimental data are taken from Refs. [6], [8], and [10], respectively. The yields are normalized to unity.

In Fig. 5 we compare the experimental [6, 8, 10] and calculated charge distributions. The agreement is good for spontaneous fission of ^{252}Cf and neutron induced fission of ^{240}Pu . In the case of ^{236}U the calculated charge number distribution appears to be shifted by two units relative to the experiment [6] towards the symmetrical charge division. The calculated distribution has a maximum at Zr, while the experimental one at Sr. But in the experiment [35] the yield has its maximum for Zr nuclides.

3.1.2. Ternary fission

The calculations show that the potential energies of ternary systems in actinides are about 20 MeV lower than in binary systems. If one assumes a direct formation of the ternary system which competes with the formation of the binary system, then ternary fission would have a larger yield than binary fission. Since this contradicts the experimental results, the ternary system is not directly formed. We assume that the binary system is formed first, and then the ternary system follows by extracting the light charged particle (LCP) into the region between the two heavy fragments. The LCP is built up from one or several alpha-particles and neutrons. Then the ternary system decays. In this picture the charge distribution for ternary fission is strongly ruled by the one for binary fission. Such relationships between binary and ternary charge distributions are found in the experiment [16].

Using the statistical approach, one can estimate the relative yields of ternary systems with a given LCP with (Z_3, A_3) . First, the relative probability for the formation of the binary system containing the fragments with (Z_1^b, A_1^b) and (Z_2^b, A_2^b) is calculated as follows:

$$Y_b(A_1^b, Z_1^b) = Y_b^0 \int \int \exp(-U_b(A_1^b, Z_1^b, \beta_1, A_2^b, Z_2^b, \beta_2, E^*)/T) d\beta_1 d\beta_2, \quad (7)$$

where Y_b^0 is the normalization factor and U_b the potential energy of the binary system at the minimum at $d = d_m$. The sums $A_1^b + A_2^b$ and $Z_1^b + Z_2^b$ are equal to the mass and charge numbers of the fissioning nucleus, respectively. Then, from each binary system several ternary systems with different charge and mass asymmetries can be formed by extracting one or several alpha-particles plus several neutrons from one or both fragments. The formation of the third particle between the two heavy fragments in the region of their interaction is more preferable than in any other place because such a co-axial configuration has the minimal potential energy.

Examples of the formation of ternary systems from binary ones are listed in Table 1 for ^{252}Cf . The system with the same charge asymmetry can be formed from several different binary systems. For each binary system and a certain LCP, the relative probabilities for the ternary systems are calculated:

$$Y_t(A_1, Z_1, A_3, Z_3, A_1^b, Z_1^b) = Y_t^0(A_3, Z_3, A_1^b, Z_1^b) \times \int \int \exp(-U(A_1, Z_1, \beta_1, A_2, Z_2, \beta_2, A_3, Z_3, E^*)/T) d\beta_1 d\beta_2, \quad (8)$$

where $Y_t^0(Z_3, A_3, Z_1^b, A_1^b)$ is the normalization factor. The potential energies correspond to the barriers of the interaction potential because the yields for ternary fission are of interest. To find the yield of decay of a certain ternary

system formed from a certain binary system, one should multiply the corresponding probabilities: $Y_b(Z_1^b, A_1^b) \times Y_t(Z_1, A_1, Z_3, A_3, Z_1^b, A_1^b)$. Finally, the yields are summed for the systems with the same charge asymmetries and the same LCP, and then the charge distribution is obtained:

$$Y(Z_1, A_3, Z_3) = \sum_{A_1^b, Z_1^b, A_1} Y_b(A_1^b, Z_1^b) \times Y_t(A_1, Z_1, A_3, Z_3, A_1^b, Z_1^b). \quad (9)$$

The normalization factors in (7) and (8) are chosen so that the binary yields as well as the yields of ternary systems from a certain binary system are normalized to unity. Hence, the obtained charge distribution Y is normalized to unity. The probability of formation of the alpha-particle from the heavy fragment is practically the same for all the heavy fragments considered in the present work (see [36]) and does not influence the relative yields.

Table 1

Examples of formation of ternary systems from binary ones in ^4He - and ^{10}Be -accompanied spontaneous ternary fission of ^{252}Cf

Binary system	Ternary system	Ternary system
$^{102}\text{Zr} + ^{150}\text{Ce}$	$^{98}\text{Sr} + ^4\text{He} + ^{150}\text{Ce}$	$^{92}\text{Kr} + ^{10}\text{Be} + ^{150}\text{Ce}$
	$^{102}\text{Zr} + ^4\text{He} + ^{146}\text{Ba}$	$^{98}\text{Sr} + ^{10}\text{Be} + ^{144}\text{Ba}$
		$^{102}\text{Zr} + ^{10}\text{Be} + ^{140}\text{Xe}$
$^{106}\text{Mo} + ^{146}\text{Ba}$	$^{102}\text{Zr} + ^4\text{He} + ^{146}\text{Ba}$	$^{96}\text{Sr} + ^{10}\text{Be} + ^{146}\text{Ba}$
	$^{106}\text{Mo} + ^4\text{He} + ^{142}\text{Xe}$	$^{102}\text{Zr} + ^{10}\text{Be} + ^{140}\text{Xe}$
		$^{106}\text{Mo} + ^{10}\text{Be} + ^{136}\text{Te}$

The results of the calculations for the spontaneous fission of ^{252}Cf in comparison with the experimental data are shown in Fig. 6. Since the binary system Mo+Ba has the largest yield and the potential energy of the ternary system Mo+ ^4He +Xe is smaller than for Zr+ ^4He +Ba, the ternary charge distribution with the LCP ^4He has a maximum at Mo. This is in agreement with the data of Ref. [37], where $Y(\text{Mo} + ^4\text{He} + \text{Xe})/Y(\text{Zr} + ^4\text{He} + \text{Ba})=1.6$. However, in the recent processing of the experimental data [16] the LCP ^4He seems to be extracted with a larger preference from the light fragment and the distribution has a maximum at Zr. The width of the distribution seems to be well reproduced in the present calculations.

For the LCP ^{10}Be , the maxima of the experimental and calculated distributions coincide. It should be mentioned that the distribution has a larger width than in the case of ^4He . For the ^{14}C -accompanied ternary fission, the calculated and experimental maxima again coincide, but the calculated yield at $Z_1 = 36$ is smaller than in the experiment. The width of the distribution is

larger than in the case of ^{10}Be -accompanied ternary fission. We also present the calculated charge distribution for ternary fission with the LCP ^{20}O in Fig. 6. The tendency of the increase of the width of the charge distribution with the charge of the LCP can be easily explained. If the LCP is heavier and consists of several alpha-particles, then one can form more ternary systems with different charge asymmetries from one binary system.

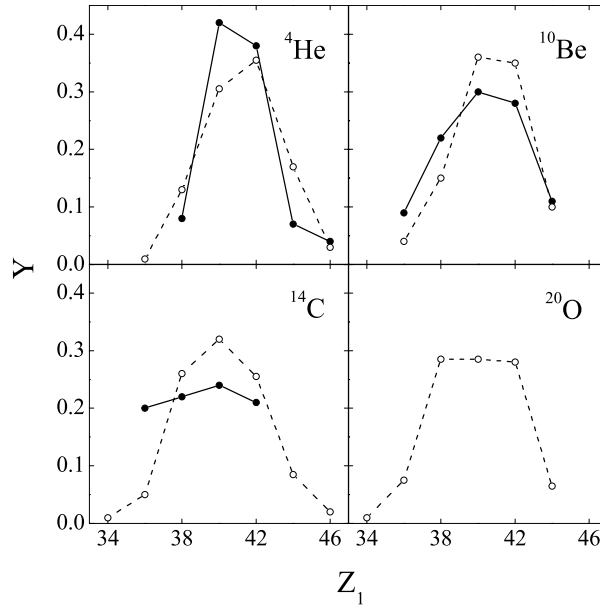


Fig. 6 – Charge distributions in spontaneous ternary fission of ^{252}Cf accompanied by the indicated LCPs. The calculated and experimental [16] points are shown by open and closed circles, respectively, connected by straight lines.

3.2. TOTAL KINETIC ENERGY OF THE FISSION FRAGMENTS

The kinetic energy of the fission fragments is an important characteristic. For binary fission we suppose that all the interaction energy of the system at scission transforms after fission into kinetic energy of the fragments:

$$\text{TKE} = V^{C,int} + V^{N,int}, \quad (10)$$

where TKE is the total kinetic energy of the fragments. In the statistical approach the mean total kinetic energy of the fragments for the fission of a

particular binary system can be calculated using the following expression:

$$\begin{aligned} \langle \text{TKE} \rangle (A_1, Z_1, A_2, Z_2) &= \\ &= \frac{\int \int \text{TKE}(\{A_i, Z_i, \beta_i\}) \exp[-U(\{A_i, Z_i, \beta_i\})/T] d\beta_1 d\beta_2}{\int \int \exp[-U(\{A_i, Z_i, \beta_i\})/T] d\beta_1 d\beta_2}. \end{aligned} \quad (11)$$

It is interesting to describe theoretically the experimental TKE-mass distributions which are the mean TKE of fission fragments as a function of mass number of one of the fragments, e.g. A_1 . To obtain the TKE-mass distribution we sum over the charge number of this fragment as follows:

$$\langle \text{TKE} \rangle (A_1) = \sum_{Z_1} \langle \text{TKE} \rangle (A_1, Z_1, A_2, Z_2). \quad (12)$$

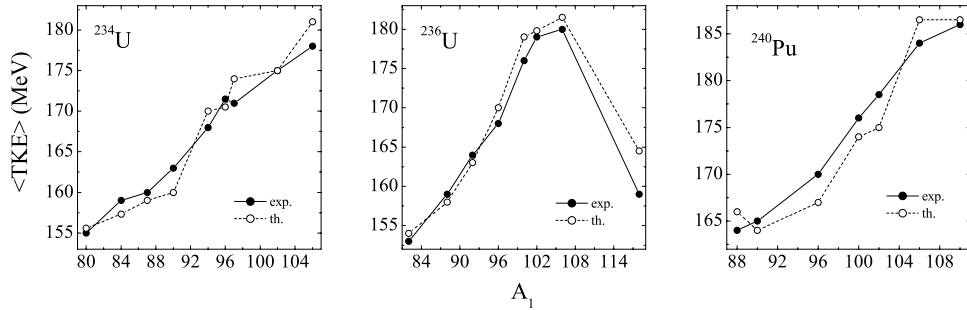


Fig. 7 – Calculated and experimental [5–8] $\langle \text{TKE} \rangle$ as a function of A_1 for neutron-induced fission of $^{234,236}\text{U}$ and ^{240}Pu . The points are connected by lines to guide the eye.

The experimentally determined fission fragments are those after neutron evaporation. The calculated quantities, however, are the primary mass and energy distributions of the fission fragments before the prompt neutron emission. In order to reconstruct the pre-neutron yield, a Monte-Carlo simulation was done in Ref. [6]. The emission of one neutron changes the kinetic energy by about 1 MeV [9]. Since for ^{234}U , ^{240}Pu and ^{250}Cf the pre-neutron yields are not presented in Refs. [5, 8, 9], the difference between the pre- and post-neutron TKEs at the same A_1 , presented for ^{236}U fission in Ref. [6], is added to the measured post-neutron TKE. Thus, the TKEs of primary fission fragments are 1–3 MeV larger than those after neutron emission and these corrected experimental values are compared with the calculated results in Fig. 7 and Table 2.

For ternary systems we calculated the total kinetic energy of the heavy fragments taking its value equal to the interaction energy at the scission point. The kinetic energy of the third particle was not taken into account here. To

Table 2

Comparison of the experimental (*exp*) [9–14] and calculated (*th*) mean TKE of pairs of fission fragments (in MeV)

Fragmentation	$\langle \text{TKE} \rangle_{exp}$	$\langle \text{TKE} \rangle_{th}$
$^{232}\text{Th} \rightarrow ^{98}\text{Sr} + ^{134}\text{Te}$	168	174
$^{232}\text{Th} \rightarrow ^{88}\text{Se} + ^{144}\text{Ba}$	158	153.5
$^{232}\text{Th} \rightarrow ^{114}\text{Ru} + ^{118}\text{Pd}$	153	159
$^{250}\text{Cf} \rightarrow ^{74}\text{Zn} + ^{176}\text{Er}$	159	164.5
$^{250}\text{Cf} \rightarrow ^{80}\text{Ge} + ^{170}\text{Dy}$	164	169
$^{250}\text{Cf} \rightarrow ^{88}\text{Kr} + ^{162}\text{Sm}$	170.5	177.5
$^{252}\text{Cf} \rightarrow ^{102}\text{Zr} + ^{150}\text{Ce}$	183	179
$^{252}\text{Cf} \rightarrow ^{106}\text{Mo} + ^{146}\text{Ba}$	189	190
$^{252}\text{Cf} \rightarrow ^{112}\text{Ru} + ^{140}\text{Xe}$	193	195
$^{252}\text{Cf} \rightarrow ^{118}\text{Pd} + ^{134}\text{Te}$	200	198
$^{252}\text{Cf} \rightarrow ^{124}\text{Cd} + ^{128}\text{Sn}$	192	198
$^{252}\text{Cf} \rightarrow ^{74}\text{Ni} + ^{178}\text{Yb}$		159
$^{258}\text{Fm} \rightarrow ^{126}\text{Sn} + ^{132}\text{Sn}$	230	229
$^{258}\text{Fm} \rightarrow ^{126}\text{Cd} + ^{132}\text{Te}$	205	198
$^{258}\text{No} \rightarrow ^{126}\text{Cd} + ^{132}\text{Xe}$	204	200.5

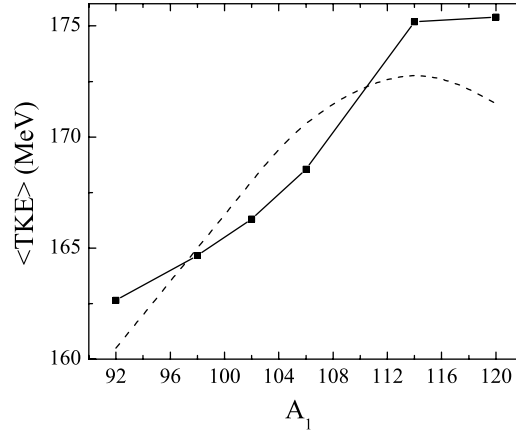


Fig. 8 – Calculated and experimental [39] $\langle \text{TKE} \rangle$ of the heavy fragments as a function of A_1 for spontaneous ^4He -accompanied fission of ^{252}Cf . The shown points are connected by lines to guide the eye. For fixed A_1 , the most probable charge splitting was found by minimizing the total energy with respect to Z_1 .

overcome the Coulomb barrier the third particle should have the kinetic energy already at scission. The mechanism of alpha-particle emission is a subject of dynamical trajectory calculations [38] and will not be discussed here. Fig. 8 shows the comparison of the calculated and experimental [39] mean

total kinetic energy of the heavy fragments in the spontaneous ternary alpha-accompanied fission of ^{252}Cf .

3.3. NEUTRON MULTIPLICITY DISTRIBUTION

Due to the excitation energy, the fission fragment can evaporate several neutrons after fission. The system at scission has the intrinsic excitation energy E^* . In the case of binary fission this energy is assumed to be divided between the fragments proportional to their level densities. Since the fragments are deformed at scission, the relaxation of the deformations to the ground-state values takes place after fission and the energies E_i^{def} of deformations are transformed into the intrinsic excitation energies E_i^* of the fragments.

$$E_i^* = E^* \frac{a_i}{a_1 + a_2} + E_i^{def}, \quad (13)$$

where a_1 and a_2 are the level density parameters of the nuclei which are expressed by the following formula [40]

$$a_i = \tilde{a}_i(A_i) \left(1 + \frac{1 - \exp\{-(E - E_c)/E_D\}}{E - E_c} \delta U_i^{sh} \right). \quad (14)$$

Here, the parameters $\tilde{a}_i(A_i)$ are taken proportional to A_i , and E_c is the energy of condensation which reduces the ground state energy of a Fermi gas by 2 MeV.

To calculate the neutron multiplicity distribution, the following expression is used:

$$\langle \nu_i \rangle = \frac{E_i^*}{B_{n_i} + 2T_i}, \quad (15)$$

where B_{n_i} is the energy of separation of the neutron and T_i is the temperature of the fragment, $T_i = (E_i^*/a_i)^{1/2}$. For small excitation energies, B_{n_i} is taken as the separation energy of the first neutron. In the case of high excitations, B_{n_i} is assumed as the average over the separation energy of the first and second neutron. The term $2T_i$ is included to describe the kinetic energy of the evaporated neutron [41].

The calculated neutron multiplicity from individual fragments in binary fission of ^{252}Cf is compared with the experimental data in Fig. 9. Since the mean kinetic energies of the fission fragments are well described with the approach presented, the calculated excitation energies of the fragments as well as the neutron multiplicities are in good agreement with the experiment [15].

Neutron multiplicity calculations for ternary fission are similar to binary ones. The excitation energy of the LCP is assumed to be small. To overcome the Coulomb barrier, the LCP obtains the energy E^{LCP} in the considered

scission configurations. Therefore, the intrinsic excitation energy of the i th heavy primary fragment ($i = 1, 2$) of the ternary fission is

$$E_i^* = (E^* - E^{LCP}) \frac{a_i}{a_1 + a_2} + E_i^{def}. \quad (16)$$

To calculate the neutron multiplicity distribution, the same expression (15) as for the binary case is used.

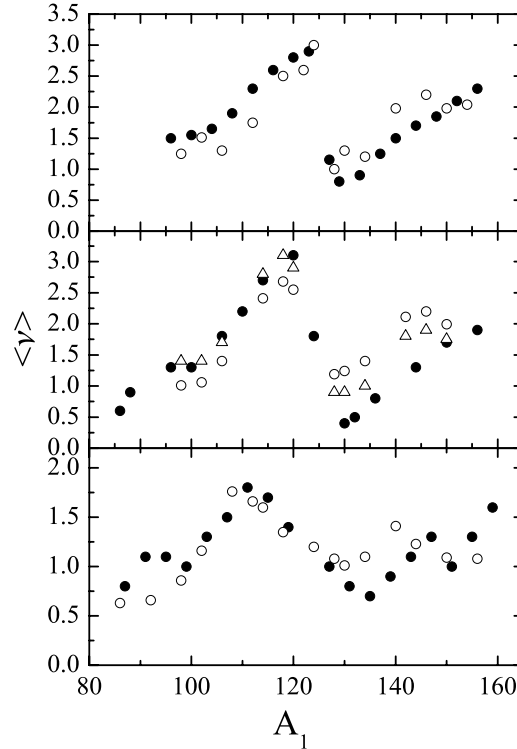


Fig. 9 – Neutron multiplicity of the fission fragments in the spontaneous binary (upper part), ${}^4\text{He}$ - (middle part) and ${}^{10}\text{Be}$ -accompanied (lower part) ternary fission of ${}^{252}\text{Cf}$ as a function of the fragment mass number A_1 . The experimental data [15] are shown by closed circles. The results, calculated with excitation energies E_1^* and E_2^* from Eq. (16) and with $E_1^* \rightarrow E_1^* - 2$ MeV and $E_2^* \rightarrow E_2^* + 2$ MeV for ${}^4\text{He}$ -accompanied fission, are presented by open circles and triangles, respectively.

In alpha-accompanied ternary fission, the TKE of the heavy fragments, which is equal to the interaction energy V^{int} at scission, is in good agreement with the experimental values as shown in Fig. 8. The alpha-particle obtains a kinetic energy E^{LCP} of about 16 MeV from the excitation energy to overcome the Coulomb barrier (this fact follows from dynamical calculations [38]). The

calculated number of neutrons emitted from the fission fragments in spontaneous alpha-accompanied ternary fission of ^{252}Cf is compared with experimental data [15] in Fig. 9. The results obtained with E_1^* and E_2^* from Eq. (16) do not so well agree with the experiment as with $E_1^* \rightarrow E_1^* - 2 \text{ MeV}$ and $E_2^* \rightarrow E_2^* + 2 \text{ MeV}$, but are still satisfactory.

For ^{10}Be -accompanied fission, the mean kinetic energy of ^{10}Be is about 18 MeV [15, 16]. But in Ref. [15] the neutron multiplicities were measured with the low energy cut-off for ^{10}Be of 26 MeV. Therefore, for comparison with the data [15] $E^{LCP} = 26 \text{ MeV}$ was taken, and we deal with data on the neutron multiplicity only for a part of ^{10}Be -accompanied fission. Note that for ^4He the cut-off is smaller than the mean kinetic energy of ^4He . Again Eqs. (14) and (16) were used in the calculation of E_i^* ($i = 1, 2$). The comparison of the calculations with the experiment is presented in Fig. 9. As in binary fission, the dependence of $\nu(A_1)$ in ternary fission looks like a “saw-tooth” curve. For ^4He and ^{10}Be as LCPs, the values of $\nu(A_1)$ are almost the same in the vicinity of $A_1 = 132$, indicating the importance of the shell structure at $Z = 50$ and $N = 82$. The present model also predicts the same “saw-tooth” curves for heavier LCPs. The quite good description of neutron multiplicities results from the possibility of the present approach to determine the excitation energies of fission fragments, as well as their kinetic energies.

4. SUMMARY

In the present work a scission-point model for the description of binary and ternary heavy nuclear fission is developed. Based on calculations of the potential energy of the fissioning system at the scission point the statistical approach reproduces the mass, charge and kinetic energy distributions for binary and ternary fission, and the neutron multiplicity distribution from fission fragments.

In binary fission the nucleus at scission is described within the dinuclear system model, which allows to set the mass and charge numbers of the fragments independently as well as their deformations. The dependence of the shell effects on deformations of the fragments plays an important role in the calculation of fission characteristics. With the potential energy of different scission configurations, we proposed a method to calculate the mass and charge distributions. The calculated results of charge distributions agree well with the experimental data. The total kinetic energy (TKE) of the fragments is assumed as the value of the interaction potential at the scission point. The experimental dependence of the mean TKE of the fission fragments on the

mass of the light fragment is well reproduced. By using the calculated excitation energies the number of neutrons emitted from each fission fragment is obtained. The dependence of the number of neutrons on the fragment mass is in a good agreement with the experimental data.

For ternary fission we developed a model analogous to the scission-point model of binary fission. The ternary fission is considered as a two-step process. In the first step the binary system is formed, in the second step the third light charged particle (LCP) originates from one or several alpha-particles and neutrons in the region of interaction between the two binary fragments. The potential energy for the ternary scission configuration is calculated analogously as in the binary case. Using the values of the energies of ternary scission configurations we obtained the probabilities for the formation of ternary systems from different binary ones. Taking into account the probabilities for the formation of binary systems we calculated the charge distributions of ternary systems for the spontaneous ternary fission of ^{252}Cf accompanied by the LCPs ^4He , ^{10}Be , ^{14}C , and ^{20}O . The results are in agreement with the experimental data. The kinetic energy of heavy fragments as well as the neutron multiplicity distributions are also well reproduced.

Acknowledgements. This work was supported by DFG (Bonn), RFBR (Moscow) and Volkswagen-Stiftung (Hannover).

REFERENCES

1. D.N. Poenaru, R.A. Gherghescu and W. Greiner, in *Proc. Int. Workshop on New Applications of Nuclear Fission*, Bucharest, 2003, Eds. A.C. Mueller, M. Mirea, and L. Tassan-Got, World Scientific, Singapore, 2004, p. 1.
2. A. Sandulescu, D.N. Poenaru, and W. Greiner, *Sov. J. Part. Nucl.*, **11**, 528 (1980).
3. B.D. Wilkins, E. P. Steinberg, and R.R. Chasman, *Phys. Rev.*, C **14**, 1832 (1976).
4. V.V. Volkov, *Izv. Akad. Nauk SSSR, Ser. Fiz.*, **50**, 1879 (1986); V.V. Volkov, *Deeply Inelastic Nuclear Reactions*, Energoatomizdat, Moscow, 1982.
5. U. Quade *et al.*, *Nucl. Phys.*, A **487**, 1 (1988).
6. W. Lang, H.G. Clerc, H. Wohlfarth, H. Schrader, and K. H. Schmidt, *Nucl. Phys.*, A **345**, 34 (1980).
7. F.J. Hamsch, H.H. Knitter, C. Budtz-Jorgensen, and J.P. Theobald, *Nucl. Phys.*, A **491**, 56 (1989).
8. C. Schmitt *et al.*, *Nucl. Phys.*, A **430**, 21 (1984).
9. R. Hentzschel, H.R. Faust, H.O. Denschlag, B.D. Wilkins, and J. Gindler, *Nucl. Phys.*, A **571**, 427 (1994).
10. G.M. Ter-Akopian *et al.*, *Phys. Rev.*, C **55**, 1146 (1997).
11. C. Budtz-Jorgensen and H.H. Knitter, *Nucl. Phys.*, A **490**, 307 (1988); A **491**, 56 (1989).
12. G. Barreau *et al.*, *Nucl. Phys.*, A **432**, 411 (1985).
13. M. Piessens, E. Jacobs, S. Pomme, and D. de Frenne, *Nucl. Phys.*, A **556**, 88 (1993).

14. E.K. Hulet *et al.*, Phys. Rev., C **40**, 770 (1989); Phys. Rev. Lett., **56**, 313 (1986).
15. M. Mutterer *et al.*, in *Proceedings of 3rd Int. Conf. on Dynamical Aspects of Nuclear Fission, Casta-Papiernicka*, Slovak Republic, 1996, edited by J. Kliman and B.I. Pustynnik, JINR, Dubna, 1996, p. 250, and references therein; M. Mutterer *et al.*, Nucl. Phys., A **738**, 122 (2004).
16. G.M. Ter-Akopian *et al.*, Physics of Atomic Nuclei, **67**, 1860 (2004).
17. A.V. Ramayya *et al.*, Rhys. Rev., C **57**, 2370 (1998).
18. J.H. Hamilton *et al.*, Prog. Part. Nucl. Phys., **38**, 273 (1997).
19. I.D. Alkhozov, B.F. Gerasimenko, A.V. Kuznetsov, B.F. Petrov, V.A. Rubchenya, and V.I. Shpakov, Sov. J. Nucl. Phys., **57**, 978 (1988).
20. S. Oberstedt *et al.*, Nucl. Phys., A **761**, 173 (2005).
21. I. Halpern, Annu. Rev. Nucl. Sci., **21**, 245 (1971).
22. N. Carjan, A. Sandulescu, and V.V. Pashkevich, Phys. Rev., C **11**, 782 (1975).
23. G.A. Pik-Pichak, Sov. J. Nucl. Phys., **40**, 215 (1984).
24. A.S. Roshchin, V.A. Rubchenya, and S.G. Yavshits, Sov. J. Nucl. Phys., **53**, 909 (1991).
25. V.A. Rubchenya and S.G. Yavshits, Z. Phys., A **329**, 217 (1988).
26. D.S. Delion, A. Florescu, and A. Sandulescu, Phys. Rev., C **63**, 044312 (2001); A. Sandulescu *et al.*, J. Phys. G., **24**, 181 (1996).
27. W.P. Myers and W. Swiatecki, Arkiv Fysik, **36**, 343 (1967).
28. V.M. Strutinsky, Nucl. Phys., A **95**, 420 (1967); A **122**, 1 (1968).
29. J. Maruhn and W. Greiner, Z. Physik, **251**, 431 (1972).
30. G. G. Adamian *et al.*, Int. J. Mod. Phys., E **5**, 191 (1996).
31. A. Krasznahorkay *et al.*, Phys. Rev. Lett., **80**, 2073 (1998); P.G. Thirolf and D. Habs, Prog. Part. Phys., **49**, 325 (2002).
32. J.F. Berger, M. Girod, and D. Gogny, Nucl. Phys., A **502**, 85c (1989); M.K. Pal, Nucl. Phys., A **556**, 201 (1993); K. Rutz *et al.*, Nucl. Phys., A **590**, 680 (1994); A. Sobczewski *et al.*, Nucl. Phys., A **473**, 77 (1987); V.V. Pashkevich, Nucl. Phys., A **169**, 275 (1971); P. Möller, S.G. Nilsson, and R.K. Sheline, Phys. Lett., B **40**, 329 (1972).
33. V.M. Strutinsky, *2nd Int. Symposium on Physics and Chemistry of Fission*, IAEA, Vienna, 1969, p. 155.
34. N.V. Antonenko, G.G. Adamian, W. Scheid, and V.V. Volkov, Nuovo Cimento, A **110**, 1143 (1997); V.V. Volkov, G.G. Adamian, N.V. Antonenko, and E.A. Cherepanov, Nuovo Cimento, A **110**, 1127 (1997); G.G. Adamian, N.V. Antonenko, W. Scheid, and V.V. Volkov, Nucl. Phys., A **633**, 409 (1998).
35. T.C. Chapman and G.A. Anzelon, Phys. Rev., C **17**, 1089 (1978).
36. A.V. Andreev, G.G. Adamian, N.V. Antonenko, S.P. Ivanova, S.N. Kuklin, W. Scheid, Eur. Phys. J., A **30**, 579 (2006).
37. M. Jandel *et al.*, in *Proc. Int. Conf. on Fission and Properties of Neutron-Rich Nuclei*, Sanibel Island, Florida, 2002, Eds. J.H. Hamilton, A.V. Ramayya, and H.K. Carter, World Scientific, Singapore, 2003, p. 448.
38. A.V. Andreev, G.G. Adamian, N.V. Antonenko, S.P. Ivanova, W. Scheid, to be published.
39. P. Fong, Phys. Rev., C **2**, 735 (1970).
40. A. V. Ignatyuk, *Statistical Properties of Excited Atomic Nuclei*, Energoatomizdat, Moscow, 1983.
41. E.A. Cherepanov and A.S. Iljinov, Nucleonika, **25**, 611 (1980).